

# 3-2 Evaluation of Uncertainty of Horn Antenna Calibration with the Frequency range of 1 GHz to 18 GHz.

SAKASAI Makoto, MASUZAWA Hiroshi, FUJII Katsumi, SUZUKI Akira, KOIKE Kunimasa, and YAMANAKA Yukio

NICT performs an EMI antenna calibration based on the Radio Law. Recently, the uncertainty of the EMI antenna measurement was evaluated with the three antenna method with a frequency coverage of 1 GHz to 18 GHz. The type of antenna under calibration is a pyramidal standard gain horn antenna. The main measurement device of the traditional antenna calibration system was a signal generator with a high-power amplifier and a microwave receiver. However, it was changed to a network analyzer providing a high dynamic range. The study about the 14 error factors revealed that the expanded uncertainty ( $k = 2$ ) were  $\pm 0.7$  dB (1 to 5.85 GHz) and  $\pm 1.1$  dB (5.85 to 18 GHz).

## Keywords

Standard Horn antenna, EMI Antenna Calibration, Uncertainty, Antenna gain, Three-antenna method, Mismatch

## 1 Introduction

In accordance with the Radio Law, NICT offers calibration services for loop antennas with a frequency coverage of 9 kHz to 30 MHz, dipole antennas with that of 30 MHz to 1,000 MHz, and horn antennas with that of 1 GHz to 18 GHz. Specifically with respect to horn antennas, in 1993 NICT developed and has since employed a calibration system based on the three-antenna method for a bandwidth of 1 GHz to 5 GHz[1]. In 1998, NICT added the 5 GHz to 18 GHz bandwidth to the coverage of calibration based on the same method, and also began evaluation of calibration uncertainty. The previous calibration system employed an antenna measurement system incorporating the use of a microwave receiver. This system made use of an external directional coupler and down-converter for a receiver, allowing for compensation of propagation loss

to extended lengths of coaxial cable. While this represented an advantage under the previous system, this feature also presented drawbacks: the IF bandwidth was fixed, so it was difficult to ensure a high S/N ratio and the dynamic range was narrow. This measurement system was recently replaced by a network analyzer offering faster measurement and securing a dynamic range of approximately 140 dB for the receiver, thus improving the range (measurement environment) by approximately 50 dB compared to the former system. For horn antennas with a frequency coverage of 1 GHz to 18 GHz, NICT currently calibrates the pyramidal horn antennas used as standard horn antennas in EMI antenna calibrations. Additionally, in light of the necessity under recent international agreements and in view of NICT's plans to obtain ISO 17025 accreditation, we have carried out evaluation of uncertainty in horn antenna calibration.

Since the degree of uncertainty varies significantly between low frequencies and high frequencies within a broad frequency range of 1 GHz to 18 GHz, we evaluated uncertainty separately for the frequency range from 1 GHz to 5.85 GHz and the frequency range from 5.85 GHz to 18 GHz. It should be noted that this evaluation of uncertainty was limited to the calibration of standard horn antennas.

## 2 Calibration system

For the calibration of horn antennas, we installed transmitting and receiving antennas at the midpoint of the longest side of NICT's large six-surface anechoic chamber [inside dimensions: 14 m (width)  $\times$  18 m (depth)  $\times$  6.4 m (height)], and positioned the antennas face-to-face at a distance apart of approximately 14.6 m, at a height of 3.5 m from the floor surface. Using the three-antenna method, we then obtained the antenna gains for three antennas simultaneously. This calibration system is illustrated in Fig. 1. For the transmission and reception system in this experiment, we use a network analyzer featuring a wide dynamic range. To ensure a high S/N ratio, we use a low-loss coaxial cable and avoid the use of an amplifier, which could cause higher harmonics and level fluctuation. The antennas are mounted on Bakelite antenna adjustment platforms (allowing for adjustment of azimuth,

elevation angle, and height) placed on blocks of foam polystyrol. A 6-dB pad is attached to the point of the coaxial cable connected to the antennas to reduce error in the reflection coefficient.

For axial alignment of the transmitting and receiving antennas, a laser generator is positioned midway between both antennas, and the laser beam is used to determine the horizontal and vertical of the antenna adjusting devices for optimum positioning. The platforms of the antenna adjusting devices are designed to enable fine adjustment of azimuth, elevation angle, and height. The coaxial cable connecting the antennas is routed along the side wall of the anechoic chamber to the backs of the antennas in order to minimize the effect of reflected waves. The network analyzer is installed in an anterior room located outside the anechoic chamber, and is connected to a PC via GP-IB. We use measurement software designed for the three-antenna method to maximize the efficiency and speed of calibration. The point of the coaxial cable to be connected to the antenna under calibration is fitted with a 6 dB pad to reduce error due to impedance mismatching within the transmission and reception system. The standard horn antennas used in the calibration system cover a frequency range of 1 GHz to 18 GHz, comprised of the following eight bands.

Band 1, with a frequency range of 1 GHz

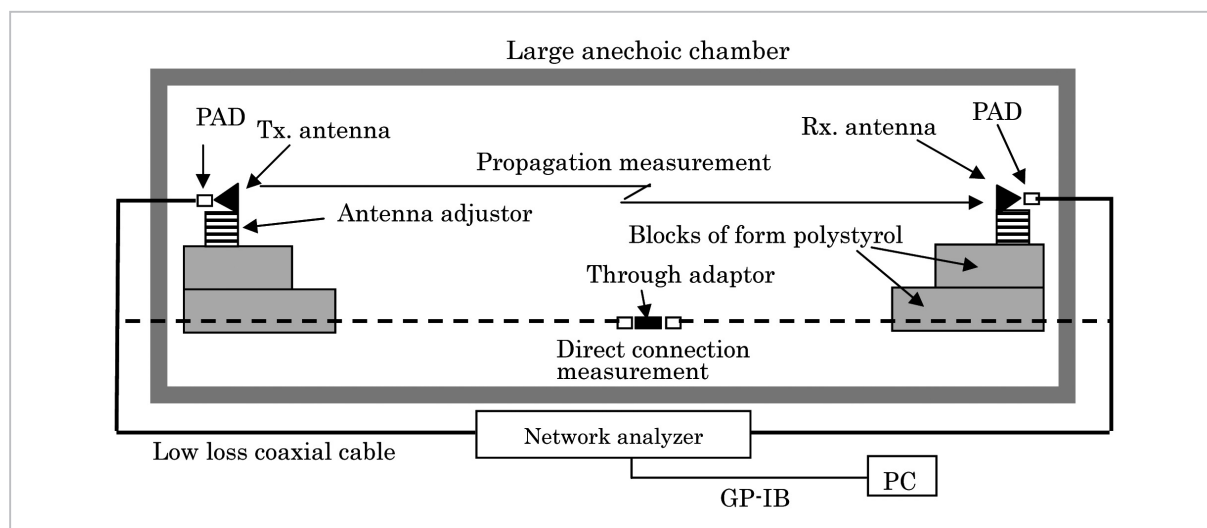


**Fig. 1** Block diagram of calibration system

to 1.15 GHz; Band 2, from 1.15 GHz to 1.7 GHz; Band 3, from 1.7 GHz to 2.6 GHz; Band 4, from 2.6 GHz to 3.95 GHz; Band 5, from 3.95 GHz to 5.85 GHz; Band 6, from 5.85 GHz to 8.2 GHz; Band 7, from 8.2 to 12.4 GHz; and Band 8, from 12.4 GHz to 18 GHz.

In our experiment, we evaluated uncertainty in two separate frequency bands: the frequency range from 1 GHz to 5.85 GHz (Band 1 through Band 5; referred to below as “Band L”) and the frequency range of 5.85 GHz to 18 GHz (Band 6 through Band 8; “Band H”).

### 3 Calibration theory and measurement method

A number of EMI antenna calibration methods are available, as follows: (1) the reference method, which uses a standard antenna as a reference for the antenna under calibration, (2) the standard field method, which determines field strength at the position of the antenna under calibration, and (3) the three-antenna method, which combines each pair of three antennas for calibration. One of the common drawbacks of methods (1) and (2) is that significant error may result if the directivities of the antennas are not identical. Method (3), on the other hand, offers an advantage in that the three antennas used in the calibration do not necessarily have to be identical; further, this method allows for calibration of any antenna capable of both transmission and reception.

Measurement of antenna gain<sup>[2]</sup> by the three-antenna method is based on the Friis transmission formula<sup>[3]</sup>. This method measures received power  $P_0$  resulting from the direct connection of the transmission and reception cable and received power  $P_{ji}$  ( $i, j = 1$  to  $3, i \neq j$ ) resulting from radio-wave emission from three different combinations of opposing antennas (#1, #2, #3).

Given the received power,  $P_{ji}$  ( $i, j = 1$  to  $3, i \neq j$ ), obtained from the pair of antenna # $i$  as a receiving antenna and antenna # $j$  as a transmitting antenna, the antenna gains of antenna

#1, #2, and #3 can be calculated by the following formulas.

$$G_1 = \frac{4\pi d}{\lambda} \sqrt{\frac{P_{21}P_{13}}{P_{23}P_0}} \quad (1)$$

$$G_2 = \frac{4\pi d}{\lambda} \sqrt{\frac{P_{23}P_{21}}{P_{13}P_0}} \quad (2)$$

$$G_3 = \frac{4\pi d}{\lambda} \sqrt{\frac{P_{13}P_{23}}{P_{21}P_0}} \quad (3)$$

where  $d$  is the distance between the transmitting and receiving antennas; this distance must remain the same in the measurement operations conducted with the three antenna combinations. The validity of the calibration results was judged by comparison with previous calibration results for NICT’s two standard horn antennas (other than the antenna under calibration).

### 4 Factors contributing to uncertainty

According to the ISO Guide dealing with uncertainty, many factors may lead to uncertainty, and these factors come into play in complex ways to produce a variety of effects<sup>[4]</sup>. These factors include: (1) definition of the quantity to be measured, (2) environmental conditions, (3) differences in values read by the individuals conducting measurement, (4) resolution or detection limit of the equipment, (5) inaccuracy of constants and parameters, (6) ambiguity of an approximation or hypothesis in the measurement method or procedure, and (7) differences arising in repeated observations of the quantity measured.

Since the system used in our experiment calibrates antenna gain based on direct-coupled measurement and propagation measurement using the three-antenna method in the anechoic chamber, measurement errors inherent in the three-antenna method contribute to uncertainty. The main causes of these errors in the three-antenna method can be classified into three groups: errors proceeding from the measurement system, errors proceeding from

the antenna setup, and measurement errors inherent in the three-antenna method.

#### 4.1.1 Errors proceeding from the measurement system

Suspected errors proceeding from the measurement system are as follows: error due to the S/N ratio, error due to the coaxial cable arrangement (specifically, bending), error in measurement stability (fluctuation over time of measured values and fluctuation due to temperature changes during measurement), and non-linearity error (i.e., level accuracy) of the measurement system.

#### 4.1.2 Errors proceeding from the antenna setup

Errors proceeding from the antenna setup include error in the distance between the opposing transmitting and receiving antennas, error in the far-field condition with the given distance between antennas, error due to dispersion in measurement of propagation loss, and error due to deviation in antenna axial alignment in the horizontal/vertical direction and in the azimuth.

#### 4.1.3 Measurement errors in the three-antenna method

Measurement errors in the three-antenna method are generated by a number of factors, as follows: error in propagation measurement due to radio-wave reflection from walls, the ceiling, and the floor (even an anechoic chamber is not a completely “free” space), error due to uncertainty in the center of radiation for the horn antenna under calibration, and errors due to mismatching among the antenna under calibration, the coaxial cable, the pad, the signal source, and the receiver.

### 4.2 Errors proceeding from the measurement system

#### 4.2.1 Error due to the S/N ratio

Two measurement techniques are employed in the three-antenna method. Direct-coupled measurement is performed by directly connecting a coaxial cable between the transmitting and receiving antennas, whereas propagation measurement is conducted by setting up both antennas for radio-wave transmission.

Since propagation measurement generates propagation loss, the level of reception falls 20 dB to 40 dB below that obtained in direct-coupled measurement. In addition, the level of reception decreases even further at higher frequencies, since coaxial cable loss is greater at higher frequencies. We measured the S/N ratio over a frequency range covering the eight bands mentioned above. Figure 2 shows an example of our measurement results. These results indicated an S/N ratio of 50.14 dB for Band L (frequency range of 1 GHz to 5.85 GHz); error (La) attributable to this S/N ratio was 0.027 dB. For Band H (frequency range of 5.85 GHz to 18 GHz), the S/N ratio was 37.9 dB and the error due to this ratio was 0.11 dB.

Error La is a Type B error unique to each measurement instrument, and uncertainty is calculated based on a rectangular distribution.

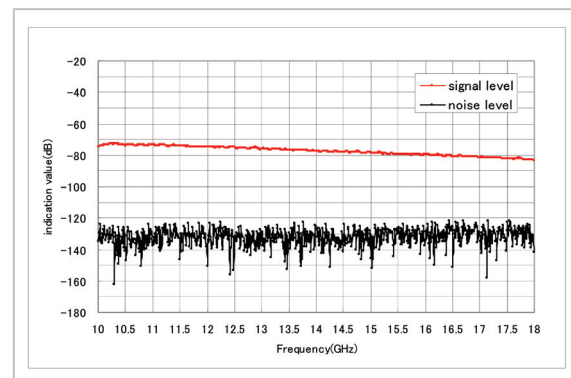


Fig.2 Error due to S/N ratio (Band 8)

#### 4.2.2 Error due to coaxial cable bend

In our experiment, the coaxial cable is routed from the network analyzer in the measurement room outside the anechoic chamber to the two opposing antennas along the wall of the anechoic chamber. The coaxial cable from the network analyzer to the antennas is laid out such that each bend had a radius of more than 50 cm, but the cable is run vertically from the connector at the coaxial waveguide converter of the antenna toward the floor. This results in a cable bend featuring a radius of approximately 10 cm near the antenna connector. To measure the effect of this cable bend, we set up an antenna such that the bending

radius was 10 cm in the horizontal direction. Example measurement results are shown in Fig. 3. Here, error (Lb) is within 0.01 dB for Band L and within 0.025 dB for Band H. This degree of error has a direct effect on the level of reception. As indicated in formulas (1) through (3), antenna gain is proportional to the square root of received power; therefore, we multiplied the obtained error value in decibels by 1/2 and multiplied this product by three, since the same error occurs in all three antennas. The error due to coaxial cable bend is a Type A error, and uncertainty is calculated based on a normal distribution.

In actual measurement, however, it is necessary to prevent bends of a radius of less than 10 cm from occurring in the cable.

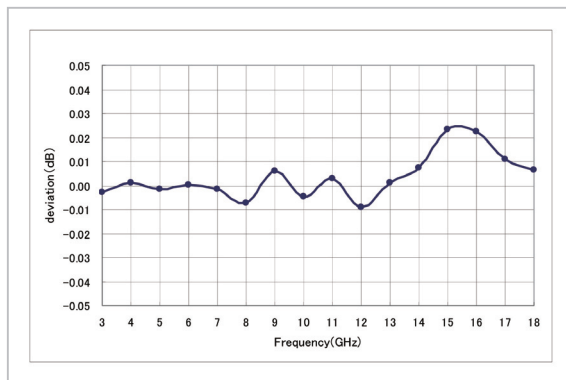


**Fig.3** Error due to coaxial cable bend

### 4.2.3 Uncertainty due to factors related to measurement system stability

#### 4.2.3.1 Error due to fluctuations over time in the measurement system

The three-antenna method requires up to around 15 minutes to complete direct-coupled measurement and propagation measurements for the three antennas. To evaluate the stability of this measurement system, we connected the coaxial cable used in the calibration and two pads, each with an attenuation level of 6 dB, to the network analyzer, and connected fixed attenuators that would simulate the actual level of propagation loss in place of the transmitting and receiving antennas. After five hours of warm-up operation of the network analyzer, level changes were measured for a

duration of 25 minutes. Although the results showed fluctuations of within 0.02 dB, we conservatively determined the error Lc due to fluctuations over time in the measurement system as 0.05 dB for both Band L and Band H. Error due to fluctuations over time in the measurement system is unique to each measurement system and is a Type B error. Uncertainty is calculated based on rectangular distribution.

#### 4.2.3.2 Error due to temperature fluctuations in the measurement system

We activated the heating/cooling apparatus in the large anechoic chamber and measurement room; after the room temperature reached approximately 20°C, we noted temperature changes using a temperature recorder. During the 15-minute period necessary for measurement based on the three-antenna method, we detected a temperature fluctuation of 0.2°C. This experiment was conducted on a cold day in December. After the measurement instrument set up for direct-coupled measurement had warmed up sufficiently, we turned on the heating/cooling apparatus in the large anechoic chamber and measurement room and observed the change in the indicated value caused by the increase in temperature. The results of measurement showed that error Ld due to these temperature changes was 0.03 dB at maximum for both Band L and Band H, even if the temperature change was estimated to be sufficiently large; i.e.,  $\pm 1^\circ\text{C}$ . The error due to temperature fluctuations in the measurement system is unique to each measurement instrument and is a Type B error. Uncertainty is calculated based on a rectangular distribution.

#### 4.2.4 Error due to non-linearity in the receiving system

We inserted a standard attenuator with a given value between Port 1 (signal source) and Port 2 (receiving side) of the network analyzer. We then measured the degree of non-linearity in the receiving system while varying the attenuation. We changed the attenuation in 10 dB increments and evaluated non-linearity based on the value indicated on the network

analyzer and the accurate attenuation value of the standard attenuator. The standard attenuator used in this measurement was a standard transfer attenuator periodically calibrated by the NMIJ (National Metrology Institute of Japan) of the AIST (National Institute of Advanced Industrial Science and Technology). The error  $L_e$  resulting from non-linearity in the receiving system was 0.04 dB for Band L and 0.05 dB for Band H. Error due to non-linearity in the receiving system is a Type B error, and uncertainty is calculated based on a rectangular distribution.

### 4.3 Errors proceeding from the antenna setup

#### 4.3.1 Error due to the antenna-to-antenna distance setting

In the measurement of antenna gain using the three-antenna method, it is important to determine the distance  $d$  between antennas with accuracy, as seen in formulas (1) through (3). In our experiment, we use a large anechoic chamber measuring 18 m in inside depth. The most suitable distance between the antenna apertures in this case is approximately 14.6 m, taking convenience into consideration; for example in terms of antenna installation. Since we used a laser range finder to measure the distance between the apertures of the transmitting and receiving antennas, high accuracy ( $\pm 1$  cm) is possible in establishing the distance between antennas. When an antenna distance of 14.6 m is set with an error of less than  $\pm 1$  cm, error  $L_f$  in antenna gain can be maintained within  $\pm 0.003$  dB for both Band L and Band H, as indicated by formulas (1) through (3). Error due to the antenna-to-antenna distance setting is a Type A error, and uncertainty is calculated based on a normal distribution.

#### 4.3.2 Error in the far-field condition

When the measuring distance is finite, measurement error results if the amplitude distribution of the surface of the wave reaching the aperture of the antenna under calibration is not uniform. When the opposing antennas are regarded as point-wave sources and the maxi-

imum aperture dimension of the test antenna is  $D$ , the distance  $d$  between the antennas resulting in measurement error of 0.05 dB or lower can be expressed by the following formula [5].

$$d \geq \frac{2D^2}{\lambda} \quad (4)$$

When the opposing antenna is a horn antenna, the distance  $d$  between the antennas can be expressed by formula (5), given that the maximum diameters of both test antenna are  $D_1$  and  $D_2$ .

$$d \geq \frac{2(D_1 + D_2)^2}{\lambda} \quad (5)$$

To suppress error to  $\leq 0.05$  dB in measurement of a standard horn antenna with a frequency coverage of Band 1 to Band 8, the minimum required distance between the antennas is 14.3 m for Band L. This requirement was satisfied by the large anechoic chamber, which allowed for a distance of up to 14.6 m between antennas. Under these measurement conditions, the error  $L_g$  in the far-field condition was  $\pm 0.048$  dB. For Band H, on the other hand, the minimum required distance between the antennas is 18.2 m, and this requirement could not be met in measurement using the large anechoic chamber. Although the required distance could be attained if the antennas were set up in the diagonal direction in the large anechoic chamber, this would result in a greater coaxial cable length and would also generate a number of other problems, such as a reduced S/N ratio. In view of the above, we decided to include the error resulting from failure to satisfy the far-field condition as a factor contributing to uncertainty. The calculation of error  $L_g$  in measurement obtained with a distance of 14.6 m between the antennas yielded a value of 0.078 dB [5]. This is a Type A error, and uncertainty is calculated based on a normal distribution.

#### 4.3.3 Error due to measurement dispersion

In the three-antenna method, propagation loss is measured three times using three different antenna combinations. We have found that

dispersion in these measurements is notably large. To evaluate this dispersion, we measured the propagation loss 22 times, by sweeping the frequencies in Band L and Band H in the large anechoic chamber under conditions equivalent to those of actual EMI antenna calibration, and calculated the standard deviation. Figures 4 and 5 show example results. Since measurement dispersion has a direct effect on the level of reception, we multiplied the obtained error value in decibels by 1/2 and multiplied the product by three, since the same error occurs in all three antennas, in the same manner as when calculating uncertainty caused by error due to a coaxial cable bend. The calculations yielded values of  $\pm 0.29$  dB for Band L and  $\pm 0.41$  dB for Band H.

This dispersion in measurement is evaluated as a Type A error, and uncertainty is calculated based on a normal distribution.

#### 4.3.4 Error in axial alignment

##### 4.3.4.1 Error in the horizontal-direction setting

For the alignment of the antenna axes, we

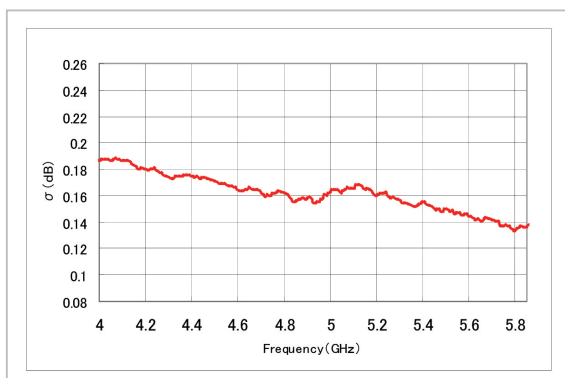


Fig.4 Measurement dispersion (Band 5)

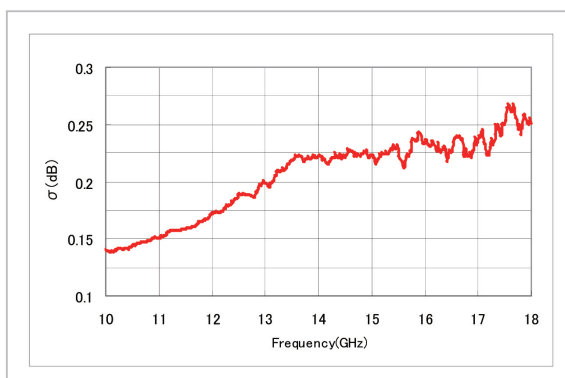


Fig.5 Measurement dispersion (Band 8)

set up a laser generator at the midpoint between the opposing antennas in the large anechoic chamber, and adjusted the positions of the antenna platforms such that the laser beam was aligned with the marks at the bottom of the apertures of the antennas. The laser generator featured a built-in level for automatic adjustment of horizontal and vertical positions, and produced a laser beam corresponding to the X-Y axis. To measure error in the horizontal-direction setting, we varied the position of the receiving antenna by a distance of 1 cm at a time (up to  $\pm 4$  cm) in the horizontal direction and measured the resultant level of reception. The results of this measurement are shown in Fig. 6. The antenna axis was adjustable within a range of  $\pm 1$  cm in the horizontal direction. Error resulting from a shift of  $\pm 1$  cm in the right or left direction was 0.05 dB for Band L and 0.17 dB for Band H. While measurement dispersion has a direct effect on the level of reception, the antenna gain is proportional to the square root of the reception level; thus we estimated error in axial alignment in the horizontal direction by multiplying the obtained error value (converted to decibels) by 1/2 and multiplied the product by three, since this measurement was conducted three times. According to our calculation results, the error  $L_i$  in the horizontal-direction axial setting was  $\pm 0.08$  dB for Band L and  $\pm 0.26$  dB for Band H. As the error due to the horizontal-direction setting is unique to each measurement instrument, it is a Type B error, and uncertainty is calculated based on a rectangular distribution.

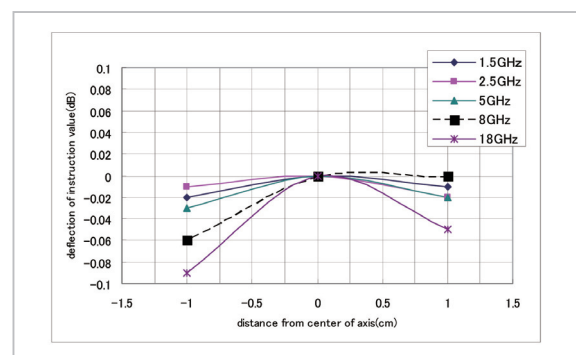
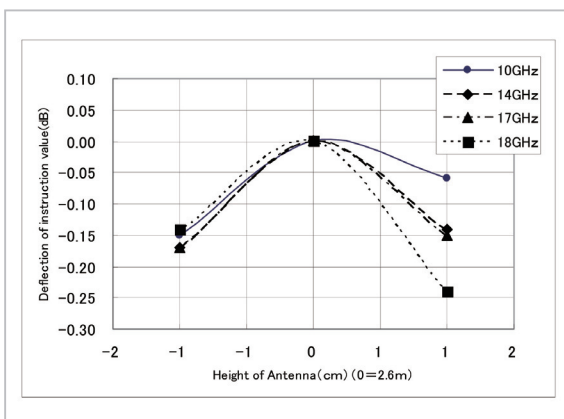


Fig.6 Example results of horizontal antenna axis alignment measurement

#### 4.3.4.2 Error in the vertical-direction setting

To measure error in the vertical-direction setting, we irradiated a laser beam from the laser generator in the direction perpendicular to the aperture of the antenna, and varied the receiving antenna height at increments of 1 cm from the center (up to  $\pm 4$  cm) in the vertical direction, and measured the resultant level of reception. The measurement results are shown in Fig. 7. The antenna axis was adjustable within a range of  $\pm 1$  cm in the vertical direction. Error resulting from a shift of  $\pm 1$  cm was  $\pm 0.09$  dB for Band L and 0.24 dB for Band H. In the same manner as calculation of error in the horizontal-direction setting, we multiplied the obtained error value (converted to decibels) by  $3/2$ . According to our calculation results, the error  $L_j$  in the vertical-direction axial setting was  $\pm 0.14$  dB for Band L and  $\pm 0.36$  dB for Band H. Error due to the vertical-direction setting is a Type B error, and uncertainty is calculated based on a rectangular distribution.



**Fig.7** Example results for vertical antenna axis alignment measurement

#### 4.3.4.3 Error due to the azimuth setting

Using the beam from a laser generator, we set up the antenna platforms such that the outer shapes of the transmitting and receiving antennas were centered. In this process, each antenna was held in place by inserting the antenna into a dedicated slit so that the azimuth could be adjusted within  $\pm 1^\circ$ . We evaluated the error in the azimuth by first

measuring the directional characteristic of the antenna and then obtaining the difference between the level obtained when the antennas were facing precisely in accordance with the stipulated characteristic ( $0^\circ$ ) and the levels obtained when there was a deviation of  $\pm 1^\circ$  to  $3^\circ$ . The results of measurement yielded values of  $\pm 0.04$  dB for Band L and  $\pm 0.24$  dB for Band H. Since error in the azimuth setting has a direct effect on the level of reception, we multiplied the obtained error value (in decibels) by  $3/2$ . According to our calculation results, the error  $L_k$  in the axial azimuth setting was  $\pm 0.06$  dB for Band L and  $\pm 0.36$  dB for Band H. Error due to the axial azimuth setting is a Type B error, and uncertainty was calculated based on a rectangular distribution.

### 4.4 Error in measurement based on the three-antenna method

#### 4.4.1 Error due to ambient reflections in the anechoic chamber

The three-antenna method conducted in a free space is designed to evaluate measurement only of the direct radio wave that is emitted from the transmitting antenna and reaches the receiving antenna. Therefore, error results when the radio wave is reflected by the floor, ceiling, wall, or antenna mounting base in the anechoic chamber, and these reflected waves are superimposed on the direct radio wave to form standing waves. To measure the effect of these reflected waves, we measured the level of reception by moving the receiving antenna tower for a total distance of approximately 50 cm. Figure 8 shows the results of 18-GHz measurement in this case, indicating error of  $\pm 0.05$  dB for Band L and  $\pm 0.09$  dB for Band H. In the same manner as for other types of error, the obtained error value (in decibels) was multiplied by  $3/2$ . According to our calculation results, error  $L_l$  due to ambient reflections in the anechoic chamber was  $\pm 0.07$  dB for Band L and  $\pm 0.14$  dB for Band H. Since the error due to ambient reflections in the anechoic chamber represents reproducible values, it is a Type A error, and uncertainty is calculated based on a normal distribution.

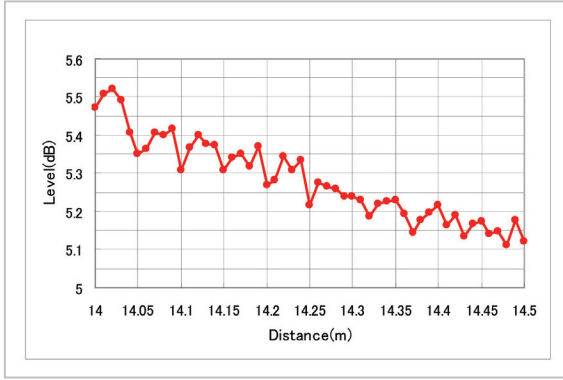


**Fig.8** Propagation characteristic (18 GHz)

#### 4.4.2 Error in the antenna center of radiation

In the three-antenna method, gain is calculated as a function of the distance between the centers of radiation of a radio wave transmitted and received by opposing antennas. However, this value is usually defined based on the distance between horn apertures, which are easier to measure. Therefore, we estimated uncertainty in this case by considering the area between the feed section and antenna aperture, where the center of radiation is located. As shown in Fig. 9, in the three-antenna method, the distance between the transmitting antenna aperture and the receiving antenna aperture is indicated as  $R$ , and the distance between the horn aperture and the feed point is indicated as  $L$ . Although the distance  $d$  between the antennas used in the calculation should be expressed as  $d = R + 2\Delta$ , which includes the distance from the radiation center of the transmitting antenna to the radiation center of the receiving antenna, we considered the area range containing the center of radiation as an

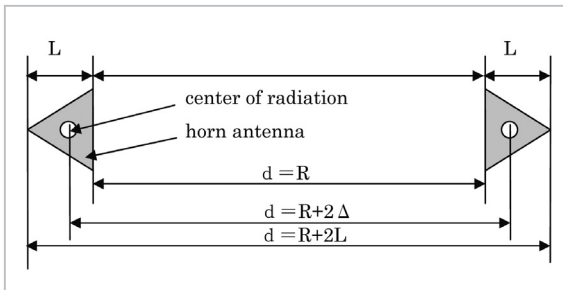


**Fig.9** Measurement distance and center of radiation used in three-antenna method

uncertainty factor, since the exact radiation center positions were unknown.

Since the center of radiation is usually located between the antenna aperture and the feed section (the apex of the horn), the value  $d$  is within the range  $R \leq d \leq R + 2L$ . Assuming the worst case, in which the center of radiation is located on the aperture plane, we performed our calculations based on the condition  $d = R$ . However, we believe that the true center of radiation is located at the farthest point behind the antenna and that the use of “ $d = R + 2L$ ” is appropriate. When “ $d = R + 2L$ ” is substituted in formula (1), the gain  $G_1$  of antenna #1 is expressed by the following formula.

$$G_1 = \frac{4\pi(R + 2L)}{\lambda} \sqrt{\frac{P_{21}P_{13}}{P_{23}P_0}} \quad (6)$$

$$= \frac{4\pi R}{\lambda} \sqrt{\frac{P_{21}P_{13}}{P_{23}P_0}} \left\{ \frac{R + 2L}{R} \right\}$$

The expression in braces represents the generated error. This is the worst value for the uncertainty resulting from the indeterminacy of the location of the center of radiation. The following formula expresses this error factor.

$$\Delta G = 10 \log_{10} \left( 1 + \frac{2L}{R} \right) \quad [\text{dB}] \quad (7)$$

According to this formula, the longer the distance  $R$  between the antennas, the less significant the antenna length  $L$  becomes, and “ $10 \log(1 + 2L/R)$ ” eventually converges to 0. In other words, if the distance  $R$  between the antennas is sufficiently large in relation to antenna dimension  $L$ , the error caused by deviation in the center of radiation becomes minimal. Figure 10 shows the results of calculations we performed using formula (7) for our study of the required distance. The horizontal axis on the graph indicates the distance  $R$  between the antenna apertures, and the vertical axis represents  $\Delta G$  in formula (7).

As indicated on the graph, when  $R$  is 10 m, for example, the worst value for uncertainty is approximately 0.2 dB even if antenna length  $L$  is 25 cm (the length of the double-ridged guide antenna, or DRGA). In practice,

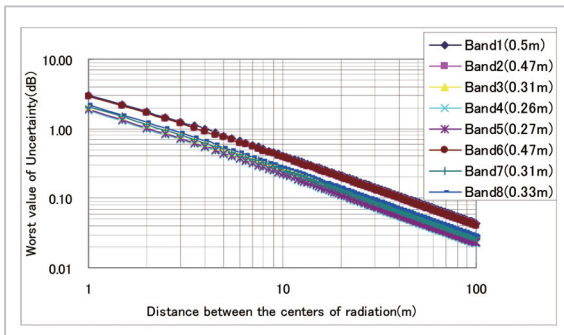


**Fig. 10** Results of calculation for center of radiation

we measured the characteristic of field strength distance by varying the distance between the antennas, obtained a regression line based on the measured characteristic, and estimated the center of radiation using the conventional method [1] (i.e., using a line extended from the regression line to estimate the center of radiation within the aperture). According to our results, error due to the deviation in the center of radiation was  $\pm 0.29$  dB for Band L and  $\pm 0.28$  dB for Band H. These values are significantly smaller than those shown in Fig. 10, and represent appropriate results. This is a Type B error, and uncertainty is calculated based on a rectangular distribution.

### 4.4.3 Error proceeding from mismatching

Using the three-antenna method, gains  $G_1$ ,  $G_2$ , and  $G_3$  of antennas #1, #2, and #3 can be calculated using formulas (1) through (3). Let us now examine the measurement of propagation loss between the transmitting and receiving antennas using antennas #1 and #2 selected from the three antennas (#1, #2, and #3). Figure 11 shows a schematic diagram of this test method. Diagram (a) shows the setup in which received power  $P_{21}$  is measured with the two connected antennas. Diagram (b) illustrates a setup in which the received power  $P_0$  is measured with antennas that are directly connected via an adaptor. The received power  $P_{21}$  obtained as shown in Fig. 11 (a) is expressed as follows when mismatching at the antenna terminal and the SG terminal are taken into consideration, in addition to loss caused by the pad and cable.

$$P_{21} = \left| \frac{C_{T21}}{1 - C_{T11}\Gamma_g} \right|^2 \left| \frac{S_{A21}^{(21)}}{(1 - S_{A11}^{(21)}\Gamma_T)(1 - S_{A22}^{(21)}\Gamma_R) - S_{A21}^{(21)}S_{A12}^{(21)}\Gamma_T\Gamma_R} \right|^2 \left| \frac{C_{R21}}{1 - C_{R22}\Gamma_L} \right|^2 P_g \quad (8)$$

Received power  $P_0$  in Fig. 11 (b) is as follows.

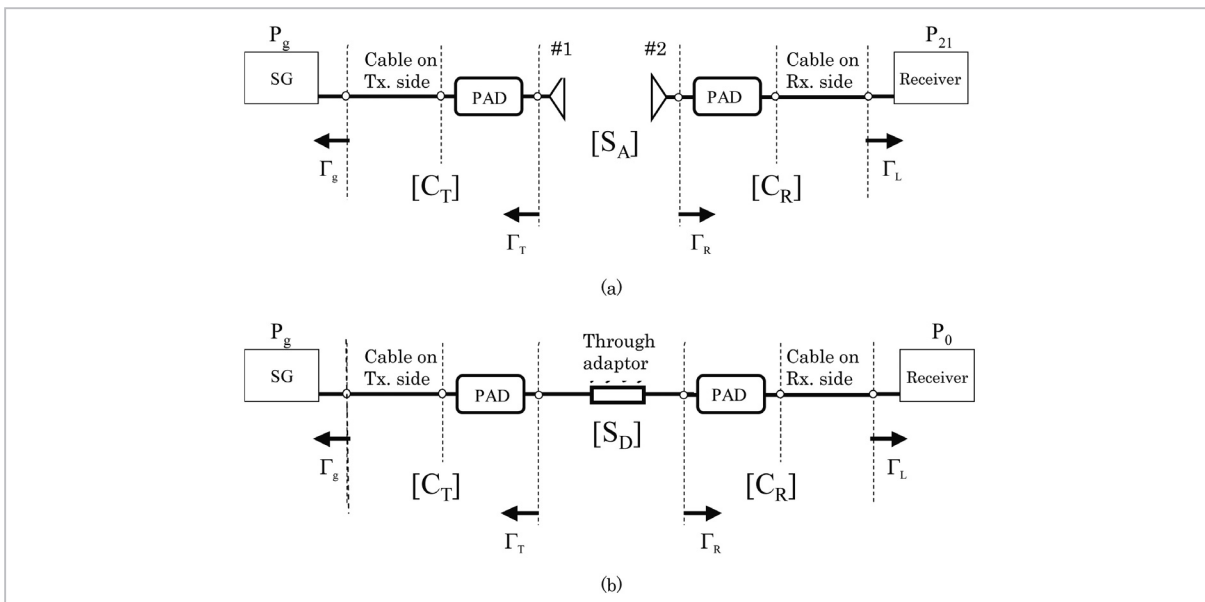


**Fig. 11** Measurement system for three-antenna method

$$P_0 = \left| \frac{C_{T21}}{1 - C_{T11}\Gamma_g} \right|^2 \left| \frac{S_{D21}}{(1 - S_{D11}\Gamma_T)(1 - S_{D22}\Gamma_R) - S_{D21}S_{D12}\Gamma_T\Gamma_R} \right|^2 \left| \frac{C_{R21}}{1 - C_{R22}\Gamma_L} \right|^2 P_g \quad (9)$$

Whereas,

- $P_g$  : Signal source output power
- $\Gamma_g$  : Signal source output reflection coefficient
- $\Gamma_L$  : Receiver input reflection coefficient
- $\Gamma_T$  : Reflection coefficient when signal source side is viewed from transmitting antenna connector
- $\Gamma_R$  : Reflection coefficient when receiver side is viewed from receiving antenna connector
- $[C_T]$  : S matrix for combination of cable on transmitting side and pad
- $[C_R]$  : S matrix for combination of cable on receiving side and pad
- $[S_D]$  : S matrix for direct-coupling connector
- $[S^{(ij)}_A]$  : S matrix between two antennas (#i  $\rightarrow$  #j)

Received power was obtained for other combinations of antennas in the same manner, and these values were substituted in formula (1), yielding the following formula.

$$G_1 = \frac{4\pi d}{\lambda} \frac{|S_{A21}^{(13)}| |S_{A21}^{(21)}|}{|S_{A21}^{(23)}|} \times \left\{ \frac{1}{|S_{D21}|} \left| \frac{(1 - S_{A11}^{(13)}\Gamma_T)(1 - S_{A22}^{(23)}\Gamma_R) - S_{A21}^{(23)}S_{A12}^{(23)}\Gamma_T\Gamma_R}{(1 - S_{D11}\Gamma_T)(1 - S_{D22}\Gamma_R) - S_{D21}S_{D12}\Gamma_T\Gamma_R} \right| \right\} \times (10)$$

In formula (10), the expression in braces indicates the factor that produces uncertainty in the calibration result. Here, five approximations are given.

- When antennas are connected and measurement is conducted,  $S_{A21}$  and  $S_{A12}$  are sufficiently smaller than 1 and multiple reflections can be ignored.
- $S_{A11}^{(13)} = S_{A11}^{(23)}$  ( $S_{A11}$  for transmitting antenna #3

remains unchanged even if the receiving antenna is changed)

- $S_{A22}^{(21)} = S_{A22}^{(23)}$  ( $S_{A22}$  for receiving antenna #2 remains unchanged even if the transmitting antenna is changed)
- $S_{D11}$  and  $S_{D22}$  for the through-adaptor are extremely small values.
- $S_{D21}$  and  $S_{D12}$  for the through-adaptor can each be assumed to equal 1.

Based on the above conditions, formula (10) can be rewritten as follows:

$$G_1 \approx \frac{4\pi d}{\lambda} \frac{|S_{A21}^{(13)}| |S_{A21}^{(21)}|}{|S_{A21}^{(23)}|} \left\{ \frac{|(1 - S_{D11}\Gamma_T)(1 - S_{D22}\Gamma_R)(1 - \Gamma_T\Gamma_R)|}{|(1 - S_{A11}^{(21)}\Gamma_T)(1 - S_{A22}^{(13)}\Gamma_R)|} \right\} \quad (11)$$

Whereas,

- $(1 - S_{A11}^{(21)}\Gamma_T)$  : Multiple reflections at the connection of antenna #1 and cable on transmitting side
- $(1 - S_{A22}^{(13)}\Gamma_R)$  : Multiple reflections at the connection of antenna #1 and cable on receiving side
- $(1 - S_{D11}\Gamma_T)$  : Multiple reflections at the connection of adaptor and cable on transmitting side
- $(1 - S_{D22}\Gamma_R)$  : Multiple reflections at the connection of adaptor and cable on receiving side
- $(1 - \Gamma_T\Gamma_R)$  : Multiple reflections between cable on transmitting side, adaptor, and cable on receiving side

Each factor in the braces in formula (11) represents the uncertainty of a U-shaped distribution. Therefore, by actually measuring the volume of each reflection coefficient, it is possible to determine uncertainty attributable to mismatching. Figure 12 shows an example of calculation of this uncertainty. It should be noted that Fig. 12 shows the results of calculation performed for each frequency. Since this error is a Type B error, uncertainty is calculated based on a U-shaped distribution.

To calculate uncertainty  $U_{\text{mismatch}}$  due to actual mismatching, we used the worst-case values in each band based on a U-shaped distribution, as shown below.

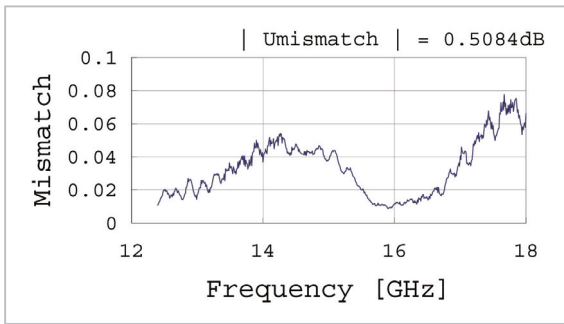


**Fig.12** Error due to mismatching (Band 8)

$$U_{mismatch} = \sqrt{|\Gamma_T|^2(|S_{D11}|^2 + |S_{A11}|^2) + |\Gamma_R|^2(|S_{D22}|^2 + |S_{A22}|^2) + |\Gamma_T|^2|\Gamma_R|^2} \quad (12)$$

## 5 Uncertainty budget

We evaluated uncertainty in the EMI antenna calibration of horn antennas with a frequency range of 1 GHz to 18 GHz using the three-antenna method. Since the antenna under calibration covered a frequency range of 1 GHz to 18 GHz in eight bands, this frequency range was divided at 5.85 GHz into Band L and Band H. Table 1 shows the uncertainty budget. Based on these results, we determined that the expanded uncertainty (coverage factor

$k = 2$ ) was  $\pm 0.7$  dB for Band L and  $\pm 1.1$  dB for Band H.

## 6 Conclusions

We examined 14 error factors that would result in uncertainty in EMI antenna calibration of a pyramidal standard gain horn antenna with a frequency coverage of 1 GHz to 18 GHz. The results of our study showed expanded uncertainty (coverage factor  $k = 2$ ) of  $\pm 0.7$  dB for Band L (1 GHz to 5.85 GHz) and  $\pm 1.1$  dB for Band H (5.85 GHz to 18 GHz).

Prior to our evaluation of uncertainty, NICT switched from its conventional antenna calibration system, which had incorporated a microwave receiver, to a new measurement system using a network analyzer. This network analyzer provides a wide dynamic range eliminating the need for the previously used directional coupler, down-converter, power amplifier, and other components; the new setup also simplified the calibration system for greater ease of use. The simplified system also enabled us to realize the concept we presently

**Table 1** Uncertainty budget for 1-GHz to 18-GHz horn antenna calibration

Uncertainty		Probability distribution	Measurement / Theory	Quantity	Uncertainty ( $\pm$ dB)		Sensitivity coefficient	Uncertainty ( $\pm$ dB)		Correction of variance	Standard uncertainty ( $\pm$ dB)		
Classification	Factor				Frequency(GHz)			Frequency(GHz)			Frequency(GHz)		
					1~5.85	5.85~18		1~5.85	5.85~18		1~5.85	5.85~18	
Measurement system	S/N ratio	Rectangular	Measurement	La	0.027	0.11	1	0.027	0.11	1/3	0.009	0.037	
	Coaxial cable bend	Normal	Measurement	Lb	0.01	0.025	(Lb/2)*3	0.015	0.04	1	0.015	0.040	
	Measurement stability	Fluctuations over time	Rectangular	Measurement	Lc	0.05	0.05	1	0.05	0.05	1/3	0.017	0.017
		Temperature fluctuations	Rectangular	Measurement	Ld	0.03	0.03	1	0.03	0.03	1/3	0.010	0.010
	Non-linearity in the receiving system	Rectangular	Measurement	Le	0.04	0.05	1	0.04	0.05	1/3	0.013	0.017	
Antenna setup	Antenna-to-antenna distance setting	Normal	Theory	Lf	0.003	0.003	1	0.003	0.003	1	0.003	0.003	
	Far-field condition	Normal	Theory	Lg	0.048	0.078	1	0.048	0.078	1	0.048	0.078	
	Measurement dispersion	Normal	Measurement	Lh	0.19	0.27	(Lh/2)*3	0.29	0.41	1	0.29	0.41	
	Axial alignment	Horizontal-direction	Rectangular	Measurement	Li	0.05	0.17	(Li/2)*3	0.08	0.26	1/3	0.027	0.087
		Vertical-direction	Rectangular	Measurement	Lj	0.09	0.24	(Lj/2)*3	0.14	0.36	1/3	0.047	0.12
Azimuth	Rectangular	Measurement	Lk	0.04	0.24	(Lk/2)*3	0.06	0.36	1/3	0.02	0.12		
Three-antenna method	Ambient reflections in the anechoic chamber	Normal	Measurement	Li	0.05	0.09	(Li/2)*3	0.07	0.14	1	0.07	0.14	
	Antenna center of radiation	Rectangular	Measurement	Lm	0.29	0.28	1	0.29	0.28	1/3	0.097	0.094	
	Mismatching	U-shaped	Measurement	Ln	0.08	0.51	1	0.08	0.51	1/2	0.040	0.255	

Combined standard uncertainty :  $U_L$  Band L (1~5.85GHz)

$$U_L = \sqrt{(0.009)^2 + (0.015)^2 + (0.017)^2 + (0.01)^2 + (0.013)^2 + (0.03)^2 + (0.048)^2 + (0.29)^2 + (0.027)^2 + (0.047)^2 + (0.02)^2 + (0.07)^2 + (0.097)^2 + (0.04)^2}$$

Combined standard uncertainty :  $U_H$  Band H (5.85~18GHz)

$$U_H = \sqrt{(0.037)^2 + (0.04)^2 + (0.017)^2 + (0.01)^2 + (0.017)^2 + (0.03)^2 + (0.078)^2 + (0.41)^2 + (0.087)^2 + (0.12)^2 + (0.12)^2 + (0.14)^2 + (0.094)^2 + (0.255)^2}$$

Uncertainty $y(k=1)$	Expanded uncertainty $U(k=2)$
0.33	0.66
0.56	1.12

apply to the evaluation of mismatch problems in high-frequency attenuators; thus, we were able to indicate the uncertainty due to mismatching clearly, using actual measurements.

Further, we focused on error in the horn antenna center of radiation and error due to mismatching. For error in the center of radiation, we varied the distance between the opposing antenna apertures by approximately 4 m and measured the propagation distance characteristic (field strength). Based on the distance characteristic, we obtained the regression line, extended that line, and estimated the center of radiation inside the aperture. This method simplified the estimation of the center of radiation based on antenna dimensions. Comparison of the results obtained by the two methods indicated that these values were very close.

The following describes precautions to be observed in EMI antenna calibration of horn antennas with a frequency coverage of 1 GHz to 18 GHz.

- (1) To minimize uncertainty in EMI antenna calibration due to inaccuracy in the center of radiation, determine the distance between antennas by estimating the center of radiation through measurement of the field strength distance characteristic or by assuming a center of radiation at the midpoint between the aperture of the antenna under calibration and the feed point.
- (2) Our study was limited to EMI antenna cal-

ibration of standard gain horn antennas. For other types of antennas of different shapes and characteristics (such as double-ridged guide antennas), it is necessary to reevaluate uncertainty by measuring directional characteristics and reflection coefficients in advance.

- (3) The characteristics of an anechoic chamber can change over time due to the aging of the wave-absorbing material used. Therefore, it is necessary to measure site attenuation periodically in order to confirm the characteristics of the anechoic chamber.
- (4) In order to minimize dispersion in measurement, it is important to handle carefully and regularly check the coaxial cable and the connecting pads used with the calibration system.

We are currently developing an EMI antenna calibration system for horn antennas with a frequency coverage of 18 GHz to 40 GHz. When this is complete, we plan to evaluate uncertainty using the method described in this paper.

## Acknowledgements

We would like to express our appreciation to Professor Akira Sugiura at Tohoku University for his kind guidance regarding EMI antenna calibration and its improvements in accuracy.

## References

- 1 H. Masuzawa, et. al., "Calibration System for 1-5 GHz-band Field Strength Meters", Review of CRL, pp. 73-81, June 1993.(in Japanese)
- 2 E.B. Larsen, R. L. Ehret D. G. Gamell, and G. H. Koepke, "Calibration of Antenna Factor at a Ground Screen Field site using an Automatic Network Analyzer", 1989, IEEE International Symp. on EMC, pp. 19-24, 1989-5.
- 3 Y. Mushiake, "Antennas and Radio Propagation", CORONA PUBLISHING, pp. 120-122, 1961. (in Japanese)
- 4 K. Iizuka, "Guide to the Expression of Uncertainty in Measurement", Japanese Standards Association, pp. 26-27, 1996. (in Japanese)
- 5 IECE, Antenna Engineering Handbook, OHMSHA, pp. 440, 1980. (in Japanese)



**SAKASAI Makoto**  
*Researcher, EMC Measurement Group,  
Wireless Communications Department  
Electromagnetic Compatibility*



**MASUZAWA Hiroshi**  
*Radio Engineering & Electronics Association  
Calibration*



**FUJII Katsumi, Dr. Eng.**  
*Researcher, EMC Measurement Group,  
Wireless Communications Department  
Electromagnetic Compatibility*



**SUZUKI Akira**  
*Senior Researcher, EMC Measurement  
Group, Wireless Communications  
Department  
Calibration*



**KOIKE Kunimasa**  
*Telecom Engineering Center  
Calibration*



**YAMANAKA Yukio**  
*Group Leader, EMC Measurement  
Group, Wireless Communications  
Department  
EMC Measurement*